An International Journal of Optimization and Control: Theories & Applications
ISSN: 2146-0957 eISSN: 2146-5703
Vol.x, No.x, pp.xx-xx (2026)
https://doi.org/10.36922/IJOCTA026160061

RESEARCH ARTICLE

Construction of minimal surfaces using trigonometric Pythagorean hodograph curves

Iqra Saeed[1], Maria Hussain[2], and Hafiz Abdul Wajid[3*]

[1]Department of Mathematics, Kinnaird College for Women, Lahore, Pakistan
[2]Department of Mathematics, Faculty of Science and Technology, Lahore College for Women University, Lahore, Pakistan
[3]Department of Electrical Engineering, Faculty of Engineering, Islamic University of Madinah, Madinah, Saudi Arabia
iqra.saeed@kinnaird.edu.pk; maria.hussain@lcwu.edu.pk; hawajid@iu.edu.sa

ARTICLE INFO

Article history:
Received: April 13, 2026
Revised: May 16, 2026
Accepted: May 20, 2026
Published Online: June 16, 2026

Keywords:
Curvature analysis
Holomorphic functions
Iso-parametric curves
Mean curvature
Surface area
Weierstrass representation

ABSTRACT

Minimal surfaces have zero mean curvature. These surfaces have the smallest possible area for a given boundary curve, and are widely used in engineering, biological design, and architecture. In this study, we present a method to construct minimal surfaces using trigonometric Pythagorean hodograph (PH) curves. First, we generate PH trigonometric curves, and subsequently apply the Weierstrass representation to derive the corresponding minimal surface. The constructed PH curve serves as a boundary isoparametric curve of the surface. We analyze key geometric properties such as symmetry, surface area and mean curvature. Representative examples are provided to demonstrate the effectiveness of the proposed method.

CC BY

1. Introduction

Minimal surfaces are surfaces with zero mean curvature and minimal area. Classic examples include planes, Enneper surfaces, and helicoids. Minimal surfaces are widely used in the design of tensile structures, ship hulls, sculptures, nanostructures, three-dimensional ball skinning, and related applications.[1–6] In computer-aided design graphics, the parametric representation of minimal surfaces is essential for practical modeling. These parametric representations of minimal surfaces enable surface upgrading and refinement via parameters to construct complex geometries. Soap film stretched across wireframes is an example of a minimal surface in everyday life.[6]

Over the years, mathematical modeling has emerged as a powerful tool in industries and digital networks.[7–11] Researchers have developed several methods for constructing intriguing surfaces with prescribed geometric properties using efficient numerical techniques (geometric modeling), including polynomial minimal surfaces. These methods include geodesic-based approximation, Weierstrass representation, harmonic and isothermal surface constructions, and partial differential equation-based approaches. Monterde[12,13] used Bézier surfaces and Dirichlet functional minimization techniques to generate minimal surfaces with prescribed boundaries. Xu and Wang[14] constructed a quintic minimal surface using the result that a surface with isothermal parameters is minimal if and only if it is harmonic. Xu et al.[15] proposed harmonic and isothermal surface construction methods for polynomial minimal surfaces of arbitrary degree, with emphasis on geometric properties and conjugate surfaces. Symmetry and shape control have also been studied.

*Corresponding Author

Alcázar and Muntingh[16] explored affine equivalence and symmetry detection in minimal surfaces. Fang et al.[17] classified polynomial minimal surfaces using shape parameters derived from Pythagorean hodograph (PH) curves. Hao and Li[18] applied Coons patches and multi-resolution analysis to satisfy boundary conditions and reduce surface area. Kassabov[19] provided general Weierstrass-based formulas for surfaces of degree five. Chen et al.[20] focused on mesh-based surface construction using area minimization fairing techniques. Güler[21] studied algebraic forms of Enneper surfaces, while Li and Zhu[22] developed biquintic minimal surfaces using holomorphic functions and parameter transformation.

Pythagorean hodograph curves, introduced by Farouki and Sakkalis,[2] are special polynomial curves whose hodographs satisfy Pythagorean conditions. These curves allow exact computation of arc length, bending energy, and offsets, which makes them suitable for machining path planning, rotation-minimizing frames, and route design.[1,2,4] Hao[23] explored the relationship between PH curves and minimal surfaces and constructed a minimal surface corresponding to a PH Bézier curve. Romani et al.[24] extended the polynomial PH curve over the six-dimensional algebraic trigonometric space to solve the C^1 Hermite interpolation problem. The defined curves exhibit the same properties as their quintic planar polynomial counterpart, such as polynomial representation of arc length and hodographs. Albrecht and Farouki[25] defined a quintic C^2 PH spline to interpolate a sequence of points and their derivative by solving a system of equations, whereas González et al.[26] extended this construction to C^2 algebraic trigonometric PH splines. Hao and Wu[27] discussed the G^1 Hermite interpolation problem for quintic-like algebraic trigonometric PH curve.

Trigonometric polynomial interpolation has also received attention for the design of smooth and aesthetic curves. Specifically, for robot path design in geometric modelling and software design in computer-aided design,[28] the trigonometric Bézier curves are extensively used. Han et al.[29] demonstrated that trigonometric methods often outperform traditional interpolation techniques. Moreover, the derivatives of trigonometric interpolation curves are smooth and continuous; therefore, these curves provide improved control and flexibility in shape design. Despite these advantages, the existing literature does not provide a framework for generating minimal surfaces whose boundaries are defined by trigonometric PH curves. This gap motivates the development of a trigonometric PH-based minimal surface scheme. The goal of this study is to present a simple and effective method that combines the geometric advantages, shape-control properties, and approximation properties of trigonometric interpolation. Important surface properties of minimal surfaces, such as symmetry, curvature, and area, are also investigated and compared with the existing literature. The main contributions of this research study are as follows:

(i) The formulation of a trigonometric PH curve based on a trigonometric interpolation scheme with flexible shape parameters.
(ii) The construction of a corresponding minimal surface whose boundary contains the derived trigonometric PH curve as an iso-parametric curve for parameter v. The isoparametric curves on the surface are obtained by taking one of the parameters (v) of the surface constant.
(iii) An analytic study of geometric properties, including symmetry, mean curvature behavior, and area.
(iv) Numerical examples showing that the proposed surface achieves significantly low mean curvature.
(v) Values of minimum, average, and maximum mean curvatures of the proposed numerical scheme are compared to the existing numerical technique,[23] which highlights that the proposed scheme produces better results.

The paper is organized as follows. In Section 2, the preliminaries of PH curves and minimal surfaces are presented. In Section 3, the trigonometric PH curve and its control points are derived. The trigonometric minimal surface is constructed in Section 4, and the conclusion is presented in Section 5.

2. Preliminaries

Definition 1.[2] A planar polynomial curve, $r(t) = (x(t), y(t))$, $r : [a, b] \rightarrow R^2$, is said to be a PH curve if and only if its derivative $r^{'}(t) = (x'(t), y'(t))$, satisfies the Pythagorean equation, $x^{'}(t)^2 + y^{'}(t)^2 = \delta(t)^2$ for some polynomial $\delta(t)$.

Here $x^{'(t)}$ *and* $y'(t)$ are the first-order derivatives of $x(t)$ *and* $y(t)$ respectively and $r^{'}(t)$ is the derivative of $r(t)$.

Remark 1. Definition 1 of the PH curve is also true for a planar trigonometric curve, i.e. a planar trigonometric curve, $r(t) = (x(t), y(t))$, $r : [a, b] \rightarrow R^2$, is a PH curve if and only if it satisfies the Pythagorean equation, $x^{'}(t)^2 + y^{'}(t)^2 = \delta(t)^2$, for some polynomial $\delta(t)$. Here $r^{'}(t)$, $x'(t)$, and

$y'(t)$ are first-order derivatives with respect to the parameter t.

The following results are of great importance for the construction of Pythagorean triples of polynomials.

Theorem 1.[30] Three real polynomials $a(t),\ b(t), c(t)$, satisfy the Pythagorean condition $a(t)^2 + b(t)^2 = c(t)^2$, if and only if they are computed as **Equation 1**:

$$\left.\begin{array}{c} a(t) = \left(k^2(t) - l^2(t)\right) m(t), \\ b(t) = 2\ k(t)\ l(t)\ m(t), \\ c(t) = \left(k^2(t) + l^2(t)\right) m(t) \end{array}\right\} \quad (1)$$

in terms of some real polynomials $k(t)$, $l(t)$, and $m(t)$.

Definition 2.[30] Let U be an open set in the complex plane C. The function $f : U \to C$ is said to be holomorphic or analytic if it is complex differentiable at every point of U.

Theorem 2.[31] Any minimal surface $\Omega : D \to R^3$, over the simply connected domain D, can be obtained as $\Omega = Re\left(\int \varphi\right)$ where $\varphi = (\varphi_1, \varphi_2, \varphi_3)$, and φ_1, φ_2 and φ_3 holomorphic functions satisfying $\varphi_1^2 + \varphi_2^2 + \varphi_3^2 = 0$.

The $\varphi_i's$ of Theorem 2 are derived by taking the values of $a(t)$, $b(t)$, and $c(t)$ from **Equation 1** and replacing t by z. Let us denote $\varphi_1 = a(z)$, $\varphi_2 = b(z)$, and $\varphi_3 = ic(z)$, then φ_i, $i = 1, 2, 3$, satisfies the Pythagorean condition $a(z)^2 + b(z)^2 = c(z)^2$ or equivalently $\varphi_1^2 + \varphi_2^2 + \varphi_3^2 = 0$.

Theorem 3.[23] For $a(z)$, $b(z)$, and $c(z)$ as defined in **Equation 1**,

$$\Omega(u, v) = Re(\int_{z_0}^{z} (a(z), b(z), ic(z))dz, \quad \text{where } z = u + iv \quad (2)$$

$\Omega(u, v)$ is a minimal surface in isothermal parameters (u, v).

These definitions were used to construct minimal surfaces in the subsequent sections. The PH trigonometric curve was computed using Definition 1 and Theorem 1. The minimal surfaces were constructed using the PH trigonometric curve, following Theorem 2 and Theorem 3.

3. Pythagorean hodograph trigonometric curve

In this section, the PH trigonometric curve is constructed using the cubic trigonometric Bézier curve.[32] The basis functions of the trigonometric Bézier curve are comprised of sine and cosine functions, which ensure smoothness. Moreover, these basis functions satisfy the properties of non-negativity, partition of unity, monotonicity and symmetry. The mathematical formula of the trigonometric Bézier curve[32] is as follows:

$$P(t) = (x(t), y(t)) = \sum_{i=0}^{3} b_i(t) P_i, \quad \mu, \rho \in [-2, 1], \quad t \in \left[0, \frac{\pi}{2}\right] \quad (3)$$

Here, $P_i's$ are the control points and $b_i(t)'s$ represent the following four basis functions.

$$\begin{aligned} b_0(t) &= (1 - \sin t)^2 (1 - \mu \sin t) \\ b_1(t) &= \sin t\ (1 - \sin t)(2 + \mu - \mu \sin t) \\ b_2(t) &= \cos t\ (1 - \cos t)(2 + \rho - \rho \cos t) \\ b_3(t) &= (1 - \cos t)^2 (1 - \rho \cos t) \end{aligned} \quad (4)$$

Here μ and ρ are the shape parameters. For $\mu, \rho = 0$, the basis functions are reduced to quadratic trigonometric polynomials. For $\mu, \rho \neq 0$, the basis functions are the cubic trigonometric polynomials. **Figure 1** illustrates the effect of variation of shape parameters on a trigonometric Bézier curve. In **Figure 1**, the interpolated data points are $\{P_i = (x_i, y_i) : -2 \leq x \leq 2\}$, which are computed from the function, $y = x^2$. **Figure 1** clearly demonstrates that the cubic trigonometric Bézier curve provides a better approximation to the original curve than the traditional cubic Bézier curve. In **Equation 3**, if $P_i = (x_i, y_i, z_i) \in R^3$, then it is a space curve, and if $P_i = (x_i, y_i) \in R^2$, $i = 0, 1, 2, 3$, then it is a planar curve.

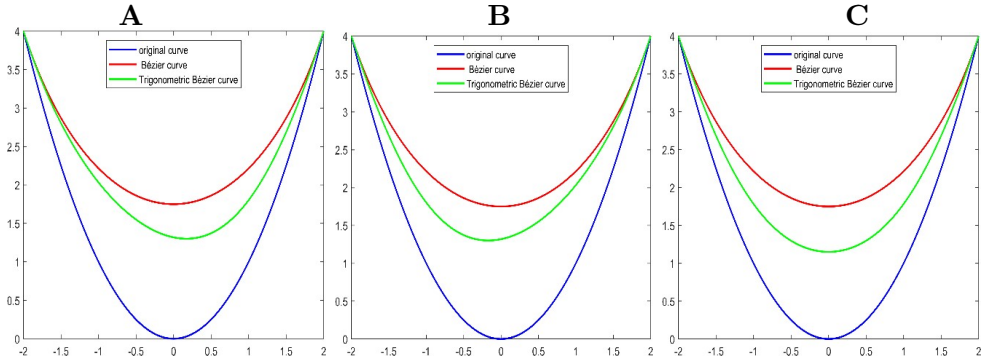


Figure 1. The effect on a cubic trigonometric Bézier curve by varying shape parameters μ and ρ. (A) $\mu = 0$ and $\rho = 1$. (B) $\mu = 1$ and $\rho = 0$. (C) $\mu = 1$ and $\rho = 1$

In this study, minimal surface construction was performed using a trigonometric Bézier curve (**Equation 3**), as trigonometric Bézier curves offer advantages over traditional Bézier curves. Since the basis functions of these curves are trigonometric functions, sines and cosines,[28] their derivatives are continuous, smooth, and non-vanishing. Trigonometric Bézier curves and trigonometric splines are extensively applied to geometric modeling of smooth approximation of robot paths, data fitting on spherical objects, and software design in computer-aided design/computer-aided manufacturing.[28]

Proposition 1. If $P_1 = P_0 + \frac{1}{6\mu}(A_1, B_1) + \frac{\mu-1}{3\mu(2+\mu)}(A_3, B_3)$, $P_2 = 2(\mu+1)P_1 - (1+2\mu)P_0 + \frac{a_0(\rho-1)}{(2+\rho)}(A_0, B_0) + \frac{1}{2}a_0(A_2, B_2)$, $P_3 = P_2 + b_0(\rho - 1)(A_0, B_0) + \frac{1}{6\rho}(A_2, B_2)$, and P_0 is arbitrarily or freely selected, then the trigonometric Bézier curve (**Equation 3**) represents the PH trigonometric curve.

Proof. Substituting the values of control points $P_i = (x_i, y_i) \in R^2$, $i = 0, 1, 2, 3$, and the derivatives of the basis functions $b_i(t)$ in **Equation 3**, the following derivatives of the parametric equations, $x(t)$ and $y(t)$, of **Equation 3** are obtained.

$$\begin{aligned} x'(t) &= \left((2+\mu) + 3\,\mu\sin^2 t\right)\cos t\ \Delta x_1 \\ &+ \left((2+\rho) + 3\rho\cos^2 t\right)\sin t\ \Delta x_3 \\ &+(-(4\mu+2)\Delta x_1 + 2\Delta x_2 \\ &-(4\ \rho+2)\Delta x_3)\sin t\cos t \end{aligned} \tag{5}$$

$$\begin{aligned} y'(t) &= \left((2+\mu) + 3\,\mu\sin^2 t\right)\cos t\ \Delta y_1 \\ &+ \left((2+\rho) + 3\rho\cos^2 t\right)\sin t\ \Delta y_3 \\ &+(-(4\mu+2)\Delta y_1 + 2\Delta y_2 \\ &-(4\ \rho+2)\Delta y_3)\sin t\cos t \end{aligned} \tag{6}$$

Here, $\Delta x_{i+1} = x_{i+1} - x_i$ and $\Delta y_{i+1} = y_{i+1} - y_i$, $i = 0, 1, 2$. The Δ represents the forward difference (see **Appendix** for derivatives of basis functions $b_i(t)$, $i = 0, 1, 2, 3$). Squaring and adding **Equations 5** and **6**, we have $\left(x'(t)\right)^2 + \left(y'(t)\right)^2 = (\delta(t))^2$, where $\delta(t)$ is a trigonometric polynomial in the variable t. Here $(\delta(t))^2 = \delta(t)\cdot\delta(t)$, and '$\cdot$' stands for dot product. $\delta(t) = \widetilde{R}_0\ cost + \widetilde{R}_1\ sint + \widetilde{R}_2\ sin^2 t\ cost + \widetilde{R}_3\ \cos^2 t\ sint + \widetilde{R}_4\ cost\ sint$, with $\widetilde{R}_0 = (\mu+2)(\Delta x_1, \Delta y_1)$, $\widetilde{R}_1 = (\rho+2)(\Delta x_3, \Delta y_3)$, $\widetilde{R}_2 = 3\mu(\Delta x_1, \Delta y_1)$, $\widetilde{R}_3 = 3\rho(\Delta x_3, \Delta y_3)$, $\widetilde{R}_4 = -(4\mu+2)(\Delta x_1, \Delta y_1) - (4\rho+2)(\Delta x_3, \Delta y_3) + 2(\Delta x_2, \Delta y_2)$, and $(\Delta x_i, \Delta y_i) \in R^2$, $i = 0, 1, 2$. (Complete expression of $(\delta(t))^2$ is given in **Appendix**).

To apply the Definition 1 and Theorem 1 to **Equations 5** and **6**, here $x'(t)$ and $y'(t)$ are represented by $a(t)$ and $b(t)$ respectively. Second, for incorporating Theorem 1, the following values of $k(t)$, $l(t)$, and $m(t)$ are judiciously selected to construct the required PH curve.

$$\begin{aligned} k(t) &= u_0\sin t + u_1\cos t, \\ l(t) &= v_0\sin t + v_1\cos t, \\ m(t) &= w_0\sin t + w_1\cos t \end{aligned} \tag{7}$$

Here, $k(t)$ and $l(t)$ are relatively prime and are not both zero for $t \in [0, \frac{\pi}{2}]$, as desired for the construction of PH curve. Here u_0 , u_1, v_0, v_1, w_0, w_1 are the free parameters and they can be any real number but they must satisfy the condition $u_0v_1 \neq u_1v_0$.

To construct the PH trigonometric curve from **Equation 7**, the values of $k(t)$, $l(t)$, and $m(t)$ are substituted into **Equation 1** as

$$\begin{aligned} a(t) &= \left((u_0\sin t + u_1\cos t)^2 - (v_0\sin t + v_1\cos t)^2\right) \\ &(w_0\sin t + w_1\cos t) \\ &= w_0\left(u_0^2 - v_0^2\right)\sin^3 t\ + w_0\left(u_1^2 - v_1^2\right)\sin t\ \cos^2 t + \\ &2w_0\left(u_0u_1 - v_0v_1\right)\sin^2 t\cos t \\ &+w_1\left(u_0^2 - v_0^2\right)\sin^2 t\cos t + w_1\left(u_1^2 - v_1^2\right)\ \cos^3 t \\ &+2w_1\left(u_0u_1 - v_0v_1\right)\ \sin t\ \cos^2 t \\ &= w_0\left(u_0^2 - v_0^2\right)\sin t\left(1 - \cos^2 t\right) + w_0\left(u_1^2 - v_1^2\right) \\ &\sin t\ \cos^2 t + 2w_0 \\ &(u_0u_1 - v_0v_1)\sin^2 t\cos t + w_1\left(u_0^2 - v_0^2\right)\sin^2 t\cos t \\ &+w_1\left(u_1^2 - v_1^2\right) \\ &\cos t\left(1 - \sin^2 t\right) + 2w_1\left(u_0u_1 - v_0v_1\right)\ \sin t\ \cos^2 t \end{aligned}$$

Similarly, $b(t)$ and $c(t)$ are calculated in the same way

$$\begin{aligned} b(t) &= 2\ (u_0\sin t + u_1\cos t)\ (v_0\sin t + v_1\cos t) \\ &(w_0\sin t + w_1\cos t), \\ c(t) &= \left((u_0\sin t + u_1\cos t)^2 + (v_0\sin t + v_1\cos t)^2\right) \\ &(w_0\sin t + w_1\cos t), \end{aligned}$$

After simplification, the following values of $x'(t) = a(t)$, $y'(t) = b(t)$ and $\delta(t) = c(t)$ are obtained.

$$\begin{aligned} a(t) &= x'(t) = A_0\sin t + (A_2 - A_0)\sin t\ \cos^2 t \\ &+(A_1 - A_3)\sin^2 t\cos t + A_3\cos t \end{aligned} \tag{8}$$

$$\begin{aligned} b(t) &= y'(t) = B_0\sin t + (B_2 - B_0)\sin t\ \cos^2 t \\ &+(B_1 - B_3)\sin^2 t\cos t + B_3\cos t \end{aligned} \tag{9}$$

$$\begin{aligned} c(t) &= \delta(t) = C_0\sin t + (C_2 - C_0)\sin t\ \cos^2 t \\ &+(C_1 - C_3)\ \sin^2 t\cos t + C_3\cos t \end{aligned} \tag{10}$$

where
$A_0 = w_0\left(u_0^2 - v_0^2\right)$,

$A_1 = w_1\left(u_0^2 - v_0^2\right) + 2w_0\left(u_0u_1 - v_0v_1\right),$
$A_2 = w_0\left(u_1^2 - v_1^2\right) + 2w_1\left(u_0u_1 - v_0v_1\right),$
$A_3 = w_1\left(u_1^2 - v_1^2\right),$
$B_0 = 2\ w_0u_0v_0,$
$B_1 = 2\ (u_0v_0w_1 + u_1v_0\ w_0 + u_0v_1w_0),$
$B_2 = 2\ (u_0v_1w_1 + u_1v_0\ w_1 + u_1v_1w_0),$
$B_3 = 2\ w_1u_1v_1,$
$C_0 = w_0\left(u_0^2 + v_0^2\right),$
$C_1 = w_1\left(u_0^2 + v_0^2\right) + 2w_0\left(u_0u_1 + v_0v_1\right),$
$C_2 = w_0\left(u_1^2 + v_1^2\right) + 2w_1\left(u_0u_1 + v_0v_1\right),$ and
$C_3 = w_1\left(u_1^2 + v_1^2\right).$

It is clear that $a(t), b(t)$, and $c(t)$ computed in **Equations 8–10** satisfy the PH condition $a(t)^2 + b(t)^2 = c(t)^2$, by construction. Comparing the coefficients of $\sin t$, $\cos t$, $\sin t\ \cos^2 t$, $\sin^2 t \cos t$ and $\sin t \cos t$, in **Equations 5** and **6** to **8** and **9**, the following system of equations is obtained:

$$(2+\mu)\Delta x_1 = A_3 \tag{11}$$

$$(2+\mu)\Delta y_1 = B_3 \tag{12}$$

$$(2+\rho)\Delta x_3 = A_0 \tag{13}$$

$$(2+\rho)\Delta y_3 = B_0 \tag{14}$$

$$3\,\mu\Delta x_1 = A_1 - A_3 \tag{15}$$

$$3\,\mu\Delta y_1 = B_1 - B_3 \tag{16}$$

$$3\rho\Delta x_3 = A_2 - A_0 \tag{17}$$

$$3\rho\Delta y_3 = B_2 - B_0 \tag{18}$$

$$-(4\mu+2)\Delta x_1 + 2\Delta x_2 - (4\ \rho+2)\Delta x_3 = 0 \tag{19}$$

$$-(4\mu+2)\Delta y_1 + 2\Delta y_2 - (4\ \rho+2)\Delta y_3 = 0 \tag{20}$$

Solving the above system of equations simultaneously, the following control points of the PH trigonometric curve are computed below: Adding **Equations 11** and **15**, we have:

$$\Delta x_1 = \tfrac{1}{2}\left(\tfrac{A_3}{2+\mu} + \tfrac{A_1 - A_3}{3\ \mu}\right) = \tfrac{A_1}{6\mu} + \tfrac{\mu-1}{3\mu(2+\mu)}A_3 \tag{21}$$

As $\Delta x_1 = x_1 - x_0$, so we have:

$$x_1 = x_0 + \tfrac{A_1}{6\mu} + \tfrac{\mu-1}{3\mu(2+\mu)}A_3 \tag{22}$$

Similarly, adding **Equations 12** and **16**, we have:

$$y_1 = y_0 + \tfrac{B_1}{6\mu} + \tfrac{\mu-1}{3\mu(2+\mu)}B_3 \tag{23}$$

From the above calculation, it follows that:

$$P_1 = P_0 + \tfrac{1}{6\mu}\left(A_1, B_1\right) + \tfrac{\mu-1}{3\mu(2+\mu)}\left(A_3, B_3\right) \tag{24}$$

where $P_1 = (x_1, y_1)$, $P_0 = (x_0, y_0)$.

Adding **Equations 13** and **17**, we have:

$$\Delta x_3 = \tfrac{1}{2}\left(\tfrac{A_0}{2+\rho} + \tfrac{A_2 - A_0}{3\ \rho}\right) = \tfrac{A_2}{6\rho} + \tfrac{\rho-1}{3\rho(2+\rho)}A_0 \tag{25}$$

As $\Delta x_3 = x_3 - x_2$, so we have:

$$x_3 = x_2 + \tfrac{A_2}{6\rho} + \tfrac{\rho-1}{3\rho(2+\rho)}A_0 \tag{26}$$

Similarly, by solving **Equations 14** and **18**, we have:

$$y_3 = y_2 + \tfrac{B_2}{6\rho} + \tfrac{\rho-1}{3\rho(2+\rho)}B_0 \tag{27}$$

It leads to the following value of the control point: $P_3 = P_2 + b_0(\rho-1)\left(A_0, B_0\right) + \frac{1}{6\rho}\left(A_2, B_2\right)$, where $b_0 = \frac{1}{3\rho(2+\rho)}$.

From **Equation 19**, we have:

$$\Delta x_2 = \tfrac{1}{2}\left((4\mu+2)\Delta x_1 + (4\ \rho+2)\Delta x_3\right) \tag{28}$$

Substituting the values of Δx_1, Δx_2, and Δx_3, we have:

$$x_2 - x_1 = (2\mu+1)\left(x_1 - x_0\right) + (2\ \rho+1)\left(x_3 - x_2\right) \tag{29}$$

$$(2\ \rho+2)x_2 = (2\mu+2)x_1 - (2\mu+1)x_0 + (2\ \rho+1)x_3 \tag{30}$$

Substituting the value of x_3, we have:

$$(2\ \rho+2)x_2 = (2\mu+2)x_1 - (2\mu+1)x_0 + (2\ \rho+1)\left(x_2 + \tfrac{A_2}{6\rho} + \tfrac{\rho-1}{3\rho(2+\rho)}A_0\right) \tag{31}$$

$$x_2 = (2\mu+2)x_1 - (2\mu+1)x_0 + (2\ \rho+1)\left(\tfrac{A_2}{6\rho} + \tfrac{\rho-1}{3\rho(2+\rho)}A_0\right) \tag{32}$$

Similarly, from **Equation 20**, we have:

$$y_2 = (2\mu+2)y_1 - (2\mu+1)y_0 + (2\ \rho+1)\left(\tfrac{B_2}{6\rho} + \tfrac{\rho-1}{3\rho(2+\rho)}B_0\right) \tag{33}$$

From x_2 and y_2, the final value of the control point P_2 is the following:

$$P_2 = 2(\mu+1)P_1 - (1+2\mu)P_0 + \tfrac{a_0(\rho-1)}{(2+\rho)}\left(A_0, B_0\right) + \tfrac{1}{2}a_0\left(A_2, B_2\right) \tag{34}$$

Here, $a_0 = \frac{2\rho+1}{3\rho}$, $b_0 = \frac{1}{3\rho(2+\rho)}$.

The complete set of control points obtained above is given below

$$P_1 = P_0 + \tfrac{1}{6\mu}\left(A_1, B_1\right) + \tfrac{\mu-1}{3\mu(2+\mu)}\left(A_3, B_3\right)$$

$$P_2 = 2(\mu+1)P_1 - (1+2\mu)P_0 + \tfrac{a_0(\rho-1)}{(2+\rho)}\left(A_0, B_0\right) + \tfrac{1}{2}a_0\left(A_2, B_2\right)$$

$$P_3 = P_2 + b_0(\rho-1)\left(A_0, B_0\right) + \tfrac{1}{6\rho}\left(A_2, B_2\right) \tag{35}$$

Here, $a_0 = \frac{2\rho+1}{3\rho}$, $b_0 = \frac{1}{3\rho(2+\rho)}$, P_i's are computed in terms of initial control point P_0 and shape parameters μ and ρ. A_i and B_i $i = 0, 1, 2, 3$ are already defined.

The desired PH trigonometric curve $P(t)$ is achieved by substituting the values of control points P_i, $i = 0, 1, 2, 3$, from **Equation 35**, in **Equation 3**. As in **Equation 35**, all the control points are represented in terms of P_0, therefore P_0 can be freely selected.

Remark 2. Here $k(t)$, $l(t)$, and $m(t)$ are chosen as linear functions of $\sin t$ and $\cos t$ with real parameters u_0 , u_1, v_0, v_1, w_0, w_1 so that **Equations 8** and **9** can be compared with **Equations 5** and **6**, by comparing the coefficients of trigonometric functions. These trigonometric functions are in the products of linear and quadratic combinations of $\sin t$ and $\cos t$ in **Equations 5** and **6**.

4. Construction of minimal surface

This section presents the construction of a minimal surface corresponding to the PH trigonometric curve computed in Section 3. The intrinsic relation between PH curves and the minimal surfaces described in Theorem 2 and Theorem 3 was used here for the construction of trigonometric minimal surfaces. The holomorphic functions $\varphi_1, \varphi_2, \varphi_3$ used for Weierstrass representation in Theorem 2 are defined in the form of $a(t)$, $b(t)$, and $c(t)$ in **Equations 8–10** for the newly defined PH trigonometric curve (**Equation 3**). The condition $\varphi_1^2 + \varphi_2^2 + \varphi_3^2 = 0$ is satisfied by the construction. Using Theorem 3, the construction is as follows: Insert the values of $a(z)$, $b(z), c(z)$ in **Equation 2** to define the integral in the form:

$$\Omega(u,v) = Re(\int \widetilde{\Omega}_1(u,v)dz,\ \int \widetilde{\Omega}_2(u,v)dz,\ i\int \widetilde{\Omega}_3(u,v)dz\ ) \tag{36}$$

where

$\widetilde{\Omega}_1(u,v) = A_0 \sin z + (A_2 - A_0)\sin z\ \cos^2 z + (A_1 - A_3)\ \sin^2 z \cos z + A_3 \cos z$,
$\widetilde{\Omega}_2(u,v) = B_0 \sin z + (B_2 - B_0)\sin z\ \cos^2 z + (B_1 - B_3)\ \sin^2 z \cos z + B_3 \cos z$, and
$\widetilde{\Omega}_3(u,v) = C_0 \sin z + (C_2 - C_0)\sin z\ \cos^2 z + (C_1 - C_3)\ \sin^2 z \cos z + C_3 \cos z$.

The explicit value of integrals $\widetilde{\Omega}_1(u,v), \widetilde{\Omega}_2(u,v)$, and $\widetilde{\Omega}_3(u,v)$ are as follows:

$\int \widetilde{\Omega}_1(u,v)dz = -A_0 \cos z - (A_2 - A_0)\ \frac{\cos^3 z}{3} + (A_1 - A_3)\ \frac{\sin^3 z}{3} + A_3 \sin z + \widetilde{\alpha}_1$,
$\int \widetilde{\Omega}_2(u,v)dz = -B_0 \cos z - (B_2 - B_0)\ \frac{\cos^3 z}{3} + (B_1 - B_3)\ \frac{\sin^3 z}{3} + B_3 \sin z + \widetilde{\alpha}_2$, and
$\int \widetilde{\Omega}_3(u,v)dz = -C_0 \cos z - (C_2 - C_0)\ \frac{\cos^3 z}{3} + (C_1 - C_3)\ \frac{\sin^3 z}{3} + C_3 \sin z + \widetilde{\alpha}_3$.

Here $\widetilde{\alpha}_j$, $j = 1, 2, 3$, are constants (complex numbers) of integration. Here, $\widetilde{\alpha}_j = \alpha_j + i\,\beta_j$, $i = \sqrt{-1}$.

Substituting the value of $z = u + iv$, the above integrals become complex functions of real parameters u and v given as:

$\int \widetilde{\Omega}_1(u,v)dz = A_0\,(-\cos u \cosh v + i \sin u \sinh v) - \frac{(A_2 - A_0)}{3}(\cos^3 u\ \cosh^3 v - 3i\ \cos^2 u\ \cosh^2 v \sin u \sinh v - 3\ \sin^2 u\ \sinh^2 v \cos u \cosh v) + i\ \sin^3 u \sinh^3 v + \frac{(A_1 - A_3)}{3}(\sin^3 u\ \cosh^3 v - i\ \cos^3 u\ \sinh^3 v - 3i\ \sin^2 u\ \cosh^2 v \cos u \sinh v - 3\ \cos^2 u\ \sinh^2 v \sin u \cosh v)\ + A_3\,(\sin u \cosh v + i \cos u \sinh v) + (\alpha_1 + i\ \beta_1)$,
$\int \widetilde{\Omega}_2(u,v)dz = B_0(-\cos u \cosh v + i \sin u \sinh v) - \frac{(B_2 - B_0)}{3}(\cos^3 u\ \cosh^3 v - 3i\ \cos^2 u\ \cosh^2 v \sin u \sinh v - 3\ \sin^2 u \sinh^2 v \cos u \cosh v) + i\ \sin^3 u \sinh^3 v + \frac{(B_1 - B_3)}{3}(\sin^3 u\ \cosh^3 v - i\ \cos^3 u\ \sinh^3 v - 3i\ \sin^2 u\ \cosh^2 v \cos u \sinh v - 3\ \cos^2 u \sinh^2 v \sin u \cosh v) + B_3\,(\sin u \cosh v + i \cos u \sinh v) + (\alpha_2 + i\beta_2)$,
$\int \widetilde{\Omega}_3(u,v)dz = C_0(-\cos u \cosh v + i \sin u \sinh v) - \frac{(C_2 - C_0)}{3}(\cos^3 u\ \cosh^3 v - 3i\ \cos^2 u\ \cosh^2 v \sin u \sinh v - 3\ \sin^2 u \sinh^2 v \cos u \cosh v) + i \sin^3 u \sinh^3 v + \frac{(C_1 - C_3)}{3}(\sin^3 u\ \cosh^3 v - i\ \cos^3 u\ \sinh^3 v - 3i\ \sin^2 u\ \cosh^2 v \cos u \sinh v - 3\ \cos^2 u \sinh^2 v \sin u \cosh v)\ +\ C_3\,(\sin u \cosh v + i \cos u \sinh v)\ + (\alpha_3 + i\beta_3)$

Substituting the values of integrals in **Equation 36**, the following minimal surface $\Omega(u,v)$ corresponding to the PH trigonometric curve is produced:

$$\Omega(u,v) = (\Omega_1(u,v), \Omega_2(u,v),\ \Omega_3(u,v)) \tag{37}$$
$\Omega_1(u,v) = Re(\int \widetilde{\Omega}_1(u,v)dz\ )$
$= -A_0 \cos u \cosh v - \frac{1}{3}(A_2 - A_0)(\cos^3 u \cosh^3 v - 3\ \cos u \cosh v \sin^2 u\ sinh^2 v\ ) + \frac{1}{3}\,(A_1 - A_3)\,(\sin^3 u\ \cosh^3 v - 3\ \sin u \cosh v \cos^2 u\ sinh^2 v\ ) + A_3 \sin u \cosh v + \alpha_1$,
$\Omega_2(u,v) = Re(\int \widetilde{\Omega}_2(u,v)dz\ )$
$= -B_0 \cos u \cosh v\ - \frac{1}{3}(B_2 - B_0)(\cos^3 u \cosh^3 v - 3\ \cos u \cosh v \sin^2 u\ sinh^2 v) + \frac{1}{3}\,(B_1 - B_3)\,(\sin^3 u\ \cosh^3 v - 3\ \sin u \cosh v \cos^2 u\ sinh^2 v\ ) + B_3 \sin u \cosh v + \alpha_2$
$\Omega_3(u,v) = Re(i \int \widetilde{\Omega}_3(u,v)dz\ )$
$= -C_0 \sin u \sinh v - \frac{1}{3}(C_2 - C_0)(-\sin^3 u\ sinh^3 v + 3\ \sin u \sinh v \cos^2 u\ cosh^2 v\ ) + \frac{1}{3}\,(C_1 - C_3)\,(\cos^3 u\ \sinh^3 v + 3\ \cos u \sinh v \sin^2 u\ cosh^2 v\ ) - C_3 \cos u \sinh v - \beta_3$.

Here α_1, α_2 and β_3 are the real constants.

The control points of the PH trigonometric Bézier curve corresponding to a minimal surface are calculated as follows:

$$P_1 = P_0+\frac{1}{6\mu}\left(A_1, B_1, iC_1\right)+\frac{\mu-1}{3\mu(2+\mu)}\left(A_3, B_3, iC_3\right),$$
$$P_2 = 2(\mu+1)P_1 - (1+2\mu)P_0 + \frac{a_0(\rho-1)}{(2+\rho)}\left(A_0, B_0, iC_0\right)+\frac{1}{2}a_0\left(A_2, B_2, iC_2\right),$$

$$P_3 = P_2+b_0(\rho-1)\left(A_0, B_0, iC_0\right)+\frac{1}{6\rho}\left(A_2, B_2, iC_2\right),$$

Here, $a_0=\frac{2\rho+1}{3\rho}$, $b_0=\frac{1}{3\rho(2+\rho)}$, $P_0=(x_0,y_0,z_0)$. P_i's are the spatial control points for constructing a minimal surface. These control points are defined in terms of the initial control point P_0, shape parameters μ, ρ, and A_j, B_j,C_j, j= 0, 1, 2,3 are defined above.

In the rest of this research paper, α_1, α_2, and β_3 are calculated by applying the interpolation condition $\Omega(0,0)=P_0$. Here $\Omega(0,0)$ is obtained by substituting $u=0$ and $v=0$ in **Equation 37**. In this way, $P_0=(x_0,y_0,z_0)$ is arbitrarily selected and α_1, α_2, and β_3 are computed as follows:

$$\begin{aligned}&\alpha_1 = x_0+\frac{2A_0+A_2}{3},\\ &\alpha_2 = y_0+\frac{2B_0+B_2}{3},\\ &\beta_3 = -z_0\end{aligned} \tag{38}$$

For the surface $\Omega(u,v)$, it can be verified by simple computation that $\Omega_{uu}(u,v)+\Omega_{vv}(u,v)=0$, or equivalently $\left(\frac{\partial^2\Omega_1}{\partial u^2},\frac{\partial^2\Omega_2}{\partial u^2},\frac{\partial^2\Omega_3}{\partial u^2}\right)+\left(\frac{\partial^2\Omega_1}{\partial v^2},\frac{\partial^2\Omega_2}{\partial v^2},\frac{\partial^2\Omega_3}{\partial v^2}\right)=(0,0,0)$ given as follows:

$\frac{\partial^2\Omega_1}{\partial u^2} = A_0\cos u\cosh v-\frac{1}{3}(A_2-A_0)(6\cos u\ \sin^2 u\ \cosh^3 v\ -3\cos^3 u\ \cosh^3 v$
$+21\cos u\cosh v\sin^2 u\ sinh^2 v-6\ \cos^3 u\cosh v\ sinh^2 v)$
$+\frac{1}{3}(A_1-A_3)(6\sin u\ \cos^2 u\ \cosh^3 v\ -3\ \sin^3 u\ \cosh^3 v-6\ \sin^3 u\ \cosh v\ sinh^2 v$
$+21\ \sin u\cosh v\cos^2 u\ sinh^2 v)-A_3\cos u\cosh v,$
$\frac{\partial^2\Omega_2}{\partial u^2} = B_0\cos u\cosh v-\frac{1}{3}(B_2-B_0)(6\cos^1 u\ \sin^2 u\ \cosh^3 v\ -3\cos^3 u\ \cosh^3 v$
$+21\cos u\cosh v\sin^2 u\ sinh^2 v-6\ \cos^3 u\cosh v\ sinh^2 v)$
$+\frac{1}{3}(B_1-B_3)(6\sin u\ \cos^2 u\ \cosh^3 v\ -3\ \sin^3 u\ \cosh^3 v-6\ \sin^3 u\ \cosh v\ sinh^2 v$
$+21\ \sin u\cosh v\cos^2 u\ sinh^2 v)-B_3\cos u\cosh v,$
$\frac{\partial^2\Omega_3}{\partial u^2} = C_0\left(\sin u\sinh v\right)+(C_0-C_2)\left(-7\cos^2 u\ \sin u\sinh v\ \cosh^2 v\right.$
$+2\sin^2 u\ \sin u\sinh v\ \cosh^2 v-2\cos^2 u\sin u\ \sinh^3 v$
$+\sin^2 u\ \sin u\ \sinh^3 v$
$+(C_1-C_3)\left(7\sin^2 u\cos u\sinh v\cosh^2 v-2\cos^3 u\ \sinh v\ \cosh^2 v\right.$
$-\cos^3 u\ \sinh^3 v\ +\ 2\sin^2 u\cos u\ \sinh^3 v)\ +$
$C_3(\cos u\sinh v),$

$\frac{\partial^2\Omega_1}{\partial v^2} = -A_0\cos u\cosh v\ -\frac{1}{3}(A_2-A_0)(6\cos^3 u\ cosh^1 v\ sinh^2 v+3\cos^3 u\ \cosh^3 v$
$-21\cos u\sin^2 u\ sinh^2 v\cosh v-6\ \cos u\cosh^3 v\sin^2 u)$
$+\frac{1}{3}(A_1-A_3)(6\sin^3 u\ \cosh^3 v\ sinh^2 v\ +3\ \sin^3 u\ \cosh^3 v+6\ \sin u\cosh^3 v\ \cos^2 u$
$-21\ \sin u\cos^2 u\ sinh^2 v\cosh v)+A_3\cos u\sinh v$
$\frac{\partial^2\Omega_2}{\partial v^2} = B_0\cos u\cosh v\ -\frac{1}{3}(B_2-B_0)(6\cos^1 u\ \sin^2 u\ \cosh^3 v\ -3\cos^3 u\ \cosh^3 v$
$+21\cos u\cosh v\sin^2 u\ sinh^2 v-6\ \cos^3 u\cosh v\ sinh^2 v)$
$+\frac{1}{3}(B_1-B_3)(6\sin u\ \cos^2 u\ \cosh^3 v\ -3\ \sin^3 u\ \cosh^3 v-6\ \sin^3 u\ \cosh v\ sinh^2 v$
$+21\ \sin u\cosh v\cos^2 u\ sinh^2 v)-B_3\cos u\cosh v,$
$\frac{\partial^2\Omega_3}{\partial v^2} = -\sin u\sinh v C_0-(C_0-C_2)\left(-7\cos^2 u\ \sin u\sinh v\ \cosh^2 v\right.$
$+2\sin^2 u\sin u\sinh v\cosh^2 v-2\cos^2 u\sin u\sinh^3 v+$
$\sin^3 u\sinh^3 v$
$-(C_1-C_3)(C_1-C_3)\left(7\sin^2 u\cos u\sinh v\cosh^2 v-\right.$
$2\cos^3 u\ \sinh v\ \cosh^2 v$
$-\cos^3 u\ \sinh^3 v\ +\ 2\sin^2 u\cos u\ \sinh^3 v)\ -$
$C_3\cos u\sinh v.$

Adding the corresponding components of $\Omega_{uu}(u,v)$ and $\Omega_{vv}(u,v)$, it is clear that the constructed surface (**Equation 37**) is a minimal surface as $\Omega_{uu}(u,v)+\Omega_{vv}(u,v)=\left(\frac{\partial^2\Omega_1}{\partial u^2},\frac{\partial^2\Omega_2}{\partial u^2},\frac{\partial^2\Omega_3}{\partial u^2}\right)+\left(\frac{\partial^2\Omega_1}{\partial v^2},\frac{\partial^2\Omega_2}{\partial v^2},\frac{\partial^2\Omega_3}{\partial v^2}\right)=\left(\frac{\partial^2\Omega_1}{\partial u^2}+\frac{\partial^2\Omega_1}{\partial v^2},\frac{\partial^2\Omega_2}{\partial u^2}+\frac{\partial^2\Omega_2}{\partial v^2},\frac{\partial^2\Omega_3}{\partial u^2}+\frac{\partial^2\Omega_3}{\partial v^2}\right)=(0,0,0)$.

In the following Proposition 2, the computed numerical method of construction of a minimal surface is summarized, and its mean curvature is calculated in Remark 4.

Proposition 2. If the control points are obtained from **Equation 35**, then the surface $\Omega(u,v)$ defined in **Equation 37** is a minimal surface with boundary $\Omega(u,0)$, where $\Omega(u,0)$ coincides with the PH trigonometric curve constructed in Section 3.

Proof. From **Equations 8–10**, the functions $a(t)$, $b(t)$, and $c(t)$ are constructed via PH representation such that $a(t)^2+b(t)^2=c(t)^2$. Extending to the complex variables $z=u+iv$, define $\varphi_1(z)=a(z)$, $\varphi_2(z)=b(z)$, $\varphi_3(z)=ic(z)$. Since $a(z)$, $b(z)$, and $c(z)$ are composed of trigonometric functions $\sin z$ and $\cos z$, they are holomorphic. Moreover, $\varphi_1^2+\varphi_2^2+\varphi_3^2=a(z)^2+b(z)^2-c(z)^2=0$. Thus, the triple $(\varphi_1,\varphi_2,\varphi_3)$ satisfies the hypotheses of the Weierstrass representation (Theorem 2). Therefore, the surface

$$\begin{aligned}&\Omega(u,v)=Re\left(\int_{z_0}^{z}\left(\varphi_1(\zeta),\ \varphi_2(\zeta),\varphi_3(\zeta)\right)\ d\zeta\ \right),\\ &z=u+iv\end{aligned} \tag{39}$$

is a minimal surface on a simply connected domain. The explicit parametrization given in **Equation 37** is obtained by evaluating these integrals; hence $\Omega(u, v)$ is minimal.

Finally, setting $v = 0$ (so $z = u \in R$) in **Equation 37**, and using $\cosh(0) = 1$ and $\sinh(0) = 0$, we obtain $\Omega(u, 0) = (x(u), y(u), 0)$ where $x(u) = \int a(u)\ du$, $y(u) = \int b(u)\ du$.

These coincide (up to constants determined by the initial control point P_0) with the parametric equations of the PH trigonometric curve constructed in Section 3. Hence, $\Omega(u, v)$ is a minimal surface whose boundary curve $\Omega(u, 0)$ is exactly the PH trigonometric curve.

Remark 3. As the trigonometric functions $\sin z$ and $\cos z$ are holomorphic functions. Therefore, $\varphi_k = \widetilde{\Omega}_k(u, v),\ k = 1, 2, 3$, being functions of $\sin z$ and $\cos z$ are also holomorphic functions.

Algorithm 1.

(i) Input: $P_0,\ u_0\ , u_1, v_0, v_1,\ w_0, w_1$.
(ii) Put the values of $P_0,\ u_0\ , u_1, v_0, v_1,\ w_0, w_1$ in **Equation 37** to construct the minimal surface.
(iii) Output: Desired trigonometric minimal surface $\Omega(u, v)$.

Remark 4. The mean curvature of the surface (**Equation 37**) is computed by the formula $H = \frac{eG-2fF+gE}{2(EG-F^2)}$, where $E = \Omega_u.\Omega_u$, $F = \Omega_u.\Omega_v$, $G = \Omega_v.\Omega_v$, $e = \Omega_{uu}.n$, $f = \Omega_{uv}.n$, and $g = \Omega_{vv}.n$. Here $\Omega_u = \frac{\partial \Omega}{\partial u}$ and $\Omega_v = \frac{\partial \Omega}{\partial v}$, are the first order derivatives and $\Omega_{uu} = \frac{\partial^2 \Omega}{\partial u^2}$, $\Omega_{vv} = \frac{\partial^2 \Omega}{\partial v^2}$, $\Omega_{uv} = \frac{\partial^2 \Omega}{\partial v\ \partial u}$ are the second order derivatives of the surface $\Omega(u, v)$. $n = \frac{\Omega_u \times \Omega_v}{|\Omega_u \times \Omega_v|}$, is the unit normal to the surface $\Omega(u, v)$.

Illustrative example 1. The minimal surface $\Omega(u, v)$ is constructed over the domain $\left[0, \frac{1}{2}\right] \times \left[0, \frac{1}{2}\right]$ using Proposition 2 with $P_0 = [1, 0, 0]$, $w_0 = 1,\ w_1 = 1, u_0 = 1,\ u_1 = -1, v_0 = 1,\ v_1 = 1$. It is one subdomain(patch) of the domain $(u, v) \in \left[0, \frac{\pi}{2}\right] \times \left[0, \frac{\pi}{2}\right]$ of the surface $\Omega(u, v)$ and this subdomain is chosen so it can be compared with the surface obtained by existing minimal surface construction technique.[23] The constructed minimal surface is shown in **Figure 2** where the boundary curve $\Omega(u, 0)$ representing the PH trigonometric curve is highlighted in red color. The boundary curve $\Omega(u, 0)$ is one of the isoparametric curve of the surface $\Omega(u, v)$, as one of the surface parameter v is kept constant i.e. $v = 0$.

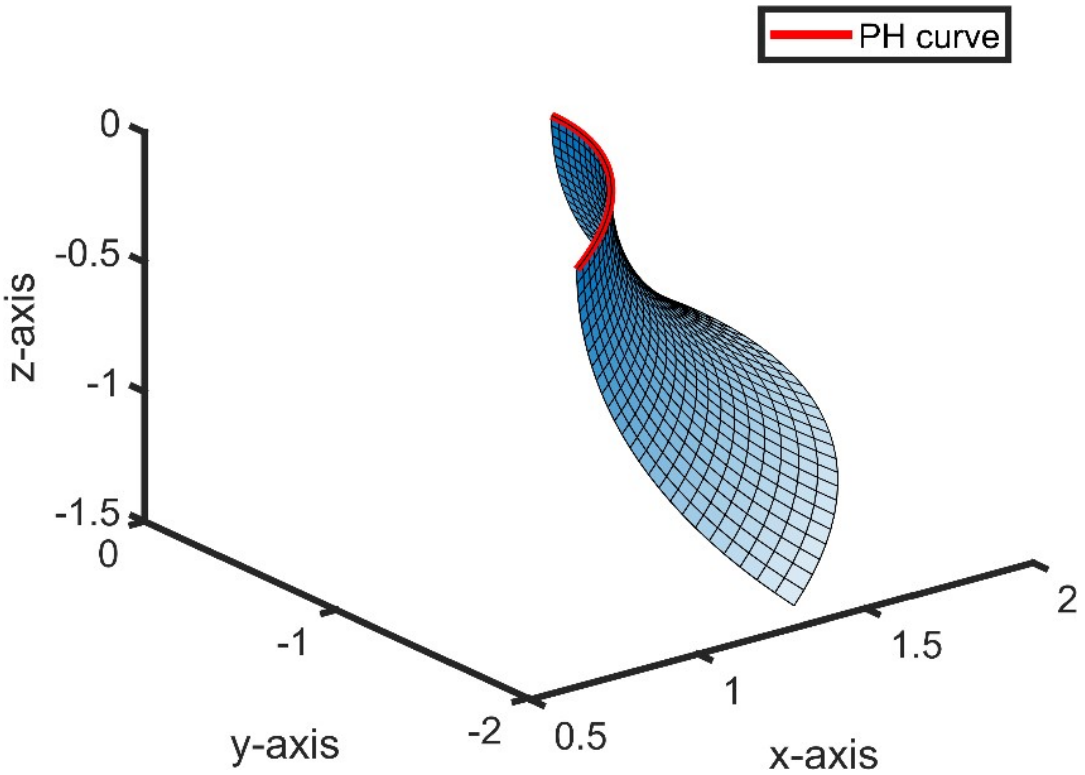


Figure 2. PH trigonometric curve (red colored) and minimal surface with $w_0 = 1$, $w_1 = 1$, $u_0 = 1$, $u_1 = -1$,$v_0 = 1$, $v_1 = 1$ and (u,v) $\in \left[0, \frac{1}{2}\right] \times \left[0, \frac{1}{2}\right]$

As domain under consideration is $\left[0, \frac{1}{2}\right] \times \left[0, \frac{1}{2}\right]$, therefore the value of the parameter u is $\left[0, \frac{1}{2}\right]$ for $\Omega(u, 0)$. The formula for computation of the mean curvature is detailed in Remark 4. For 50×50 sampling points over the domain $\left[0, \frac{1}{2}\right] \times \left[0, \frac{1}{2}\right]$, the minimum, maximum, and average values of

the mean curvature of the computed minimal surface (**Figure 2**) were calculated. The comparison of the mean curvature values of the proposed surface with the minimal surface construction scheme given in[23] is shown in **Table 1**. The table clearly shows that the mean curvature values obtained through the proposed scheme are lower than those of the other method.[23] This comparison highlights the efficiency of the proposed scheme.

Table 1. Comparison of mean curvatures

Method	**Domain specifications**	**Minimum mean curvature min($\|\mathbf{H}\|$)**	**Average mean curvature Avg($\|\mathbf{H}\|$)**	**Maximum mean curvature max($\|\mathbf{H}\|$)**
Proposed Method (Section 4)	Minimal surface with PH trigonometric curve for the domain $\left[0,\frac{1}{2}\right]\times\left[0,\frac{1}{2}\right]$	0	0.0560	0.1832
Polynomial minimal surface[23]	Polynomial minimal surface with PH curve for the domain $\left[0,\frac{1}{2}\right]\times[0,\frac{1}{2}]$	0	0.4869	2.0065

Furthermore, the computational efficiency of the proposed scheme was assessed by measuring its runtime. The proposed method required 0.3134 seconds for $P_0=[1,0,0],\ w_0=1,\ w_1=1, u_0=1,\ u_1=-1, v_0=1,\ v_1=1.$

In the following Proposition 3, the symmetry of the surface is discussed.

Proposition 3. The minimal surface $\Omega(u,v)$ derived in **Equation 37** is symmetric about the plane $Z=0(XY\text{-plane})$.

Proof. In **Equation 37**, $\Omega_1(u,v)$, $\Omega_2(u,v)$, and $\Omega_3(u,v)$ are the X, Y, and Z components of the surface $\Omega(u,v)$ i.e. $X(u,v)=\Omega_1(u,v)$, $Y(u,v)=\Omega_2(u,v)$, and $Z(u,v)=\Omega_3(u,v)$.

Replace v by $-v$ in $\Omega_1(u,v)$, $\Omega_2(u,v)$, and $\Omega_3(u,v)$ defined in **Equation 37**, it can be easily verified by simple calculation that $X(u,-v)=X(u,v), Y(u,-v)=Y(u,v), Z(u,-v)=-Z(u,v)$. Hence, the minimal surface $\Omega(u,v)$ is symmetric about the XY-plane or $Z=0$ plane with respect to the parameters v only, parameter u remains unchanged.

The area of the minimal surface is computed in Proposition 4.

Proposition 4. The approximation of the area of the minimal surface $\Omega(u,v)$ derived in **Equation 37** is 2.33948 square units, for $(u,v)\in\left[0,\frac{1}{2}\right]\times\left[0,\frac{1}{2}\right]$.

Proof. The area of the minimal surface $\Omega(u,v)$, for $(u,v)\in\left[0,\frac{1}{2}\right]\times\left[0,\frac{1}{2}\right]=D_1$(say) was evaluated using the Dirichlet functional (D) defined in previous work,[12,13] where $D=\iint_{D_1}\frac{1}{2}(E(u,v)+G(u,v))du\ dv$, $E=\Omega_u.\Omega_u$, $G=\Omega_v.\Omega_v$, *and* u,v are isothermal parameterization. By simple integration in D, the computed approximation of the area of the minimal surface is 2.33948 square units.

Remark 5. The area of a surface can be calculated by the formula, $Area=\int_R(EG-F^2)^{\frac{1}{2}}\ du\ dv$, over the real domain $R=[a,b]\times[c,d]$.[12] Here, E,G, and F are the coefficients of the first fundamental form of the surface. Due to the high non-linearity of the area functional, it was replaced in[12,13] by Dirichlet functional as $(EG-F^2)^{\frac{1}{2}}\leq(EG)^{\frac{1}{2}}\leq\frac{E+G}{2}$. As $(EG-F^2)^{\frac{1}{2}}\leq\frac{E+G}{2}$, therefore it follows that $\int_R(EG-F^2)^{\frac{1}{2}}\ du\ dv\leq\int_R\frac{(E+G)}{2}\ du\ dv$. Therefore $\int_R\frac{(E+G)}{2}\ du\ dv$ was used to approximate the area of the surface, as it does not give any disinformation (does not calculate the area of the surface less than the actual area of the computed surface). Thus. $\int_R\frac{(E+G)}{2}\ du\ dv$ was used to approximate the upper bound of the area of the minimal surface in **Figure 2**.

Remark 6. Different trigonometric minimal surfaces are constructed by **Equation 37** for different choices of free parameters $w_0,\ w_1,u_0,\ u_1,v_0,\ v_1$ over different subdomains (**Figure 3**).

In **Figure 3D**, the minimal surface (**Equation 37**) is constructed for the whole domain $\left[0,\frac{\pi}{2}\right]\times\left[0,\frac{\pi}{2}\right]$ with $w_0=2,\ w_1=2, u_0=1,\ u_1=1, v_0=1,\ v_1=-1$. The computed value of minimum mean curvature, average mean curvature and the maximum mean curvature for the minimal surface in **Figure 3D** are zero, 1.23×10^{-17}, and 1.43×10^{-16} respectively.

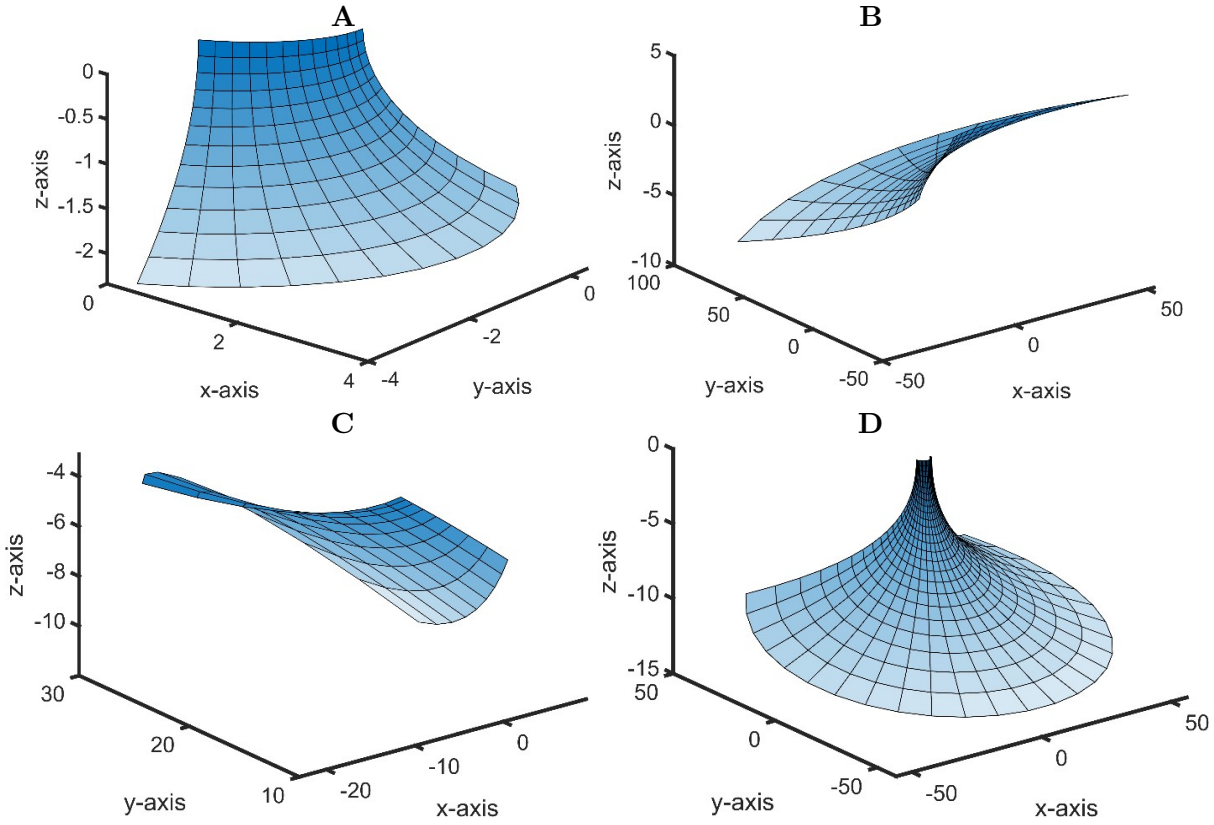


Figure 3. Different trigonometric minimal surfaces. (A) Minimal surface with $w_0 = 1$, $w_1 = 1$, $u_0 = 1$, $u_1 = -1$, $v_0 = 1$, $v_1 = 1$, and (u,v) $\in \left[0, \frac{\pi}{4}\right] \times \left[0, \frac{\pi}{4}\right]$. (B) Minimal surface with $w_0 = 2,\ w_1 = -3, u_0 = 1,\ u_1 = -1, v_0 = -1,\ v_1 = -1$, and $(u, v) \in \left[\frac{\pi}{4}, \frac{\pi}{2}\right] \times \left[\frac{\pi}{4}, \frac{\pi}{2}\right]$. (C) Minimal surface with $w_0 = 1,\ w_1 = 2, u_0 = -2,\ u_1 = 2, v_0 = 1,\ v_1 = 2$, and $(u, v) \in \left[\frac{\pi}{6}, \frac{\pi}{3}\right] \times \left[\frac{\pi}{6}, \frac{\pi}{3}\right]$. (D) Minimal surface with $w_0 = 2,\ w_1 = 2,\ u_0 = 1,\ u_1 = 1, v_0 = 1,\ v_1 = -1$, and $(u, v) \in \left[0, \frac{\pi}{2}\right] \times \left[0, \frac{\pi}{2}\right]$.

The computed values of minimum mean curvature, average mean curvature and maximum mean curvature for the minimal surface in **Figure 3** are summarized in **Table 2**. All computations and visualizations were performed using MATLAB 2023 software for programming.

Table 2. Summary of mean curvatures corresponding to different examples

Figures	**Domain**	**Minimum mean curvature min ($\|\mathbf{H}\|$)**	**Average mean curvature Avg($\|\mathbf{H}\|$)**	**Maximum mean curvature max($\|\mathbf{H}\|$)**
Figure 3A	$\left[0, \frac{\pi}{4}\right] \times \left[0, \frac{\pi}{4}\right]$	0	0.0615	0.1833
Figure 3B	$[\frac{\pi}{4}, \frac{\pi}{2}\ ] \times [\frac{\pi}{4}, \frac{\pi}{2}\ ]$	4.294×10^{-6}	0.0026	0.0174
Figure 3C	$[\frac{\pi}{6}, \frac{\pi}{3}\ ] \times [\frac{\pi}{6}, \frac{\pi}{3}\ ]$	5.156×10^{-4}	0.0167	0.0783
Figure 3D	$\left[0, \frac{\pi}{2}\right] \times \left[0, \frac{\pi}{2}\right]$	0	1.43×10^{-17}	1.25×10^{-16}

5. Conclusions

This study presents a novel and effective method for constructing minimal surfaces using trigonometric PH curves. The generated PH curve serves as a boundary isoparametric curve of the minimal surface, derived from the Weierstrass representation. The geometric properties of the resulting surfaces, including symmetry, surface area, and mean curvature, have been analyzed. The calculated surface area was 2.33948 square units, suggesting potential for material efficiency in applications such as membrane structures and aesthetic design.

This study explored the generation of minimal surfaces corresponding to trigonometric PH curves; however, in the future, it can be extended to different directions:

(i) Solving the Plateau problem where the boundary is prescribed by trigonometric PH curves.
(ii) Constructing minimal surface blends generated from multiple trigonometric PH curves defined along shared boundaries, suitable for surface blending in geometric design. The boundary of each surface patch is defined by the trigonometric PH curve, and blending multiple patches with common boundaries satisfies required continuity conditions. The continuity conditions, such as C^1 and C^2 need to be considered between adjacent patches.

Acknowledgments

The authors extend their appreciation to the Deanship of Scientific Research at the Islamic University of Madinah, Saudi Arabia, for supporting this research.

Funding

None.

Conflict of interest

The authors declare no conflict of interest.

Author contributions

Conceptualization: All authors
Formal analysis: Iqra Saeed, Maria Hussain
Investigation: Iqra Saeed, Maria Hussain
Methodology: Iqra Saeed, Maria Hussain
Writing – original draft: All authors
Writing – review & editing: All authors

Availability of data

All data analyzed have been presented in the paper.

AI tools statement

Not applicable.

References

1. Farouki RT, Giannelli C, Sestini A. New developments in theory, algorithms, and applications for Pythagorean-hodograph curves. In: Giannelli C, Speleers H, eds. *Advanced Methods for Geometric Modeling and Numerical Simulation*. Springer International Publishing; 2019:127-177. https://doi.org/10.1007/978-3-030-27331-6_7
2. Farouki RT, Sakkalis T. Pythagorean hodographs. *IBM J Res Dev*. 1990;34(5):736-752. https://doi.org/10.1147/rd.345.0736
3. Li C, Wang R, Zhu C. Designing approximation minimal parametric surfaces with geodesics. *Appl Math Model*. 2013;37(9):6415-6424. https://doi.org/10.1016/j.apm.2013.01.035
4. Shah MA, Aouf N. 3D cooperative Pythagorean hodograph path planning and obstacle avoidance for multiple UAVs. In: *2010 IEEE 9th International Conference on Cybernetic Intelligent Systems*. IEEE; 2010:1-6. https://doi.org/10.1109/UKRICIS.2010.5898124
5. Wang Y. Periodic surface modelling for computer aided nano design. *Comput Aided Des*. 2007;39(3):179-189. https://doi.org/10.1016/j.cad.2006.09.005
6. Xu G, Rabczuk T, Güler E, Wu Q, Hui KC, Wang G. Quasi-harmonic Bézier approximation of minimal surfaces for finding forms of structural membranes. *Comput Struct*. 2015;161:55-63. https://doi.org/10.1016/j.compstruc.2015.09.002
7. Solouma E, Alsulami M, Baskonus HM, Aljohani AF, Saber S. On the stochastic simulation by optimal control and bifurcation analysis of the computer virus model in Caputo-type. *Alex Eng J*. 2026;144:12-22. https://doi.org/10.1016/j.aej.2026.04.017
8. Almutairi N, Messaoudi M, Almalki FMK, Saber S. A deterministic and stochastic fractional-order model for computer virus propagation with Caputo-Fabrizio derivative: analysis, numerics, and dynamics. *CMES*. 2026;146(3):1-10. https://doi.org/10.32604/cmes.2026.076371
9. Almutairi N, Saber S. Application of a time-fractal fractional derivative with a power-law kernel to the Burke-Shaw system based on Newton's interpolation polynomials. *MethodsX*. 2024;12:102510. https://doi.org/10.1016/j.mex.2023.102510
10. Almalki FMK, Solouma E, Yavuz M, Saber S, Sarrah A. Analytical and numerical study of bifurcations and reaction-diffusion patterns in a predator-prey model with Holling-III response and variable carrying capacity. *Ain Shams Eng J*. 2026;17(6):104131. https://doi.org/10.1016/j.asej.2026.104131
11. Ahmed KIA, Adam HDS, Almutairi N, Saber S. Analytical solutions for a class of variable-order fractional Liu system under time-dependent variable coefficients. *Results Phys*. 2024;56:107311. https://doi.org/10.1016/j.rinp.2023.107311
12. Monterde J. Bézier surfaces of minimal area: the Dirichlet approach. *Comput Aided Geom Des*. 2004;21(2):117-136. https://doi.org/10.1016/j.cagd.2003.07.009
13. Monterde J. The Plateau-Bézier problem. In: *Mathematics of Surfaces (Lecture Notes in Computer Science)*. Springer Berlin Heidelberg; 2003:262-273. https://doi.org/10.1007/978-3-540-39422-8_18
14. Xu G, Wang G. Parametric polynomial minimal surfaces of degree six with isothermal parameter. In: *Lecture Notes in Computer Science*. Springer Berlin Heidelberg; 2008:329-343. https://doi.org/10.1007/978-3-540-79246-8_25

15. Xu G, Zhu Y, Wang G, Galligo A, Zhang L, Hui KC. Explicit form of parametric polynomial minimal surfaces with arbitrary degree. *Appl Math Comput*. 2015;259:124-131. https://doi.org/10.1016/j.amc.2015.02.065
16. Alcázar JG, Muntingh G. Affine equivalences of surfaces of translation and minimal surfaces, and applications to symmetry detection and design. *J Comput Appl Math*. 2022;411:114206. https://doi.org/10.1016/j.cam.2022.114206
17. Fang L, Peng Y, Li Y, Cao J. Classification of polynomial minimal surfaces. *Comput Aided Geom Des*. 2022;96:102106. https://doi.org/10.1016/j.cagd.2022.102106
18. Hao Y, Li CJ. The C^1 and C^2 quasi-Plateau problems. *J Comput Appl Math*. 2018;329:106-124. https://doi.org/10.1016/j.cam.2017.04.039
19. Kassabov O. Polynomial minimal surfaces of degree five. *Bull Math Soc Sci Math*. 2017;60(108):195-206. https://bulletin.ssmr.ro/volumes/60-2/node10.html
20. Chen W, Cai Y, Zheng J. Constructing triangular meshes of minimal area. *Comput Aided Des Appl*. 2008;5(1-4):508-518. https://doi.org/10.3722/cadaps.2008.508-518
21. Güler E. Family of Enneper minimal surfaces. *Mathematics*. 2018;6(12):281. https://doi.org/10.3390/math6120281
22. Li C, Zhu C. The classification of bi-quintic parametric polynomial minimal surfaces. *Appl Math J Chin Univ*. 2017;32(1):14-26. https://doi.org/10.1007/s11766-017-3451-2
23. Hao Y. A new method to construct polynomial minimal surfaces. *Comput Appl Math*. 2020;39(4). https://doi.org/10.1007/s40314-020-01324-2
24. Romani L, Saini L, Albrecht G. Algebraic-trigonometric Pythagorean-hodograph curves and their use for Hermite interpolation. *Adv Comput Math*. 2014;40(5-6):977-1010. https://doi.org/10.1007/s10444-013-9338-8
25. Albrecht G, Farouki RT. Construction of C^2 Pythagorean-hodograph interpolating splines by the homotopy method. *Adv Comput Math*. 1996;5(1):417-442. https://doi.org/10.1007/bf02124754
26. González C, Albrecht G, Paluszny M, Lentini M. Design of C^2 algebraic-trigonometric Pythagorean hodograph splines with shape parameters. *Comput Appl Math*. 2016;37(2):1472-1495. https://doi.org/10.1007/s40314-016-0404-y
27. Hao YX, Wu D. G^1 Hermite interpolation by planar quintic-like algebraic-trigonometric Pythagorean-hodograph curves. *J Comput Appl Math*. 2026;474:116972. https://doi.org/10.1016/j.cam.2025.116972
28. Choubey N, Ojha A. Constrained curve drawing using trigonometric splines having shape parameters. *Comput Aided Des*. 2007;39(12):1058-1064. https://doi.org/10.1016/j.cad.2007.06.005
29. Han X. Piecewise trigonometric Hermite interpolation. *Appl Math Comput*. 2015;268(1):616-627. https://doi.org/10.1016/j.amc.2015.06.125
30. Farouki RT. *Pythagorean-Hodograph Curves: Algebra and Geometry Inseparable*. 1st ed. Springer Berlin Heidelberg; 2008.
31. Nitsche JCC. *Lectures on Minimal Surfaces: Introduction, Fundamentals, Geometry and Basic Boundary Value Problems*. 1st ed. Cambridge University Press; 1989.
32. Han X, Ma Y, Huang X. The cubic trigonometric Bézier curve with two shape parameters. *Appl Math Lett*. 2009;22(2):226-231. https://doi.org/10.1016/j.aml.2008.03.015

Appendix

(i) Consider the basis functions given in **Equation 4**:

$b_0(t) = (1-\sin t)^2 (1- \ \mu \sin t)$,
$b_1(t) = \sin t \ \ (1-\sin t)(2+\mu-\mu \sin t)$,
$b_2(t) = \cos t \ \ (1-\cos t)(2+\rho-\rho \cos t)$,
$b_3(t) = (1-\cos t)^2 (1- \ \rho \cos t), t \in \left[0, \frac{\pi}{2}\right]$.

The derivatives of the basis functions are given below:

$$b_0^{'}(t) = -cost \ \ (1-\sin t)(2+\mu-3\mu \sin t),$$

$$b_1^{'}(t) = \cos t \left(-\mu \sin t (1-\sin t) + (1-2\sin t)(2+\mu-\mu \sin t)\right),$$

$$b_2^{'}(t) = \sin t \left(\rho \cos t (1-\cos t) + (-1+2\cos t)(2+\rho-\rho \cos t)\right),$$

$$b_3^{'}(t) = \sin t \ \ (1-\cos t)(2+\rho-3\rho \cos t).$$

(ii) $\delta(t) = \widetilde{R}_0 \ cost + \widetilde{R}_1 \ sint + \widetilde{R}_2 \ sin^2 t \ cost + \widetilde{R}_3 \ \cos^2 t \ sint + \widetilde{R}_4 \ cost \ sint$,
with $\widetilde{R}_0 = (\mu+2)(\Delta x_1, \Delta y_1)$, $\widetilde{R}_1 = (\rho+2)(\Delta x_3, \Delta y_3)$, $\widetilde{R}_2 = 3\mu(\Delta x_1, \Delta y_1)$,
$\widetilde{R}_3 = 3\rho(\Delta x_3, \Delta y_3)$, $\widetilde{R}_4 = -(4\mu+2)(\Delta x_1, \Delta y_1) - (4\rho+2)(\Delta x_3, \Delta y_3) + 2(\Delta x_2, \Delta y_2)$.

$$(\delta(t))^2 = R_0 \cos^2 t + R_1 \sin^2 t + R_2 \sin^4 t \ cos^2 t + R_3 \cos^4 t \ sin^2 t$$
$$+ (R_4 + 2R_{10} + 2R_6)\cos^2 t \ sin^2 t + 2R_5 costsint + 2R_7 \cos^3 t \ sint$$
$$+2R_8 sint \ cos^2 t + 2R_9 \sin^3 t \ cost + +2R_{11} \sin^2 t \ cost + 2R_{12} \sin^3 t \ \cos^3 t$$
$$+2R_{13} \sin^3 t \ \cos^2 t + 2R_{14} \sin^2 t \ \cos^3 t$$

with

$R_0 = \widetilde{R}_0 \bullet \widetilde{R}_0 = (\mu+2)^2 \left(\Delta x_1^2 + \Delta y_1^2\right)$,
$R_1 = \widetilde{R}_1 \bullet \widetilde{R}_1 = (\rho+2)^2 \left(\Delta x_3^2 + \Delta y_3^2\right)$,
$R_2 = \widetilde{R}_2 \bullet \widetilde{R}_2 = 9\mu^2 \left(\Delta x_1^2 + \Delta y_1^2\right)$,

$$R_3 = \widetilde{R}_3 \bullet \widetilde{R}_3 = 9\rho^2 \left(\Delta x_3^2 + \Delta y_3^2\right),$$

$R_4 = \widetilde{R}_4 \bullet \widetilde{R}_4 = (4\mu+2)^2 \left(\Delta x_1^2 + \Delta y_1^2\right) + (4\rho+2)^2 \left(\Delta x_3^2 + \Delta y_3^2\right) + 4\left(\Delta x_2^2 + \Delta y_2^2\right) + (32\mu\rho + 16\mu + 16\rho + 8)(\Delta x_1 \Delta x_3 + \Delta y_1 \Delta y_3) - (16\mu+8)(\Delta x_1 \Delta x_2 + \Delta y_1 \Delta y_2) - (16\rho+8)(\Delta x_2 \Delta x_3 + \Delta y_2 \Delta y_3)$,
$R_5 = \widetilde{R}_0 \bullet \widetilde{R}_1 = (\mu+2)(\rho+2)(\Delta x_1 \Delta x_3 + \Delta y_1 \Delta y_3)$,

$$R_6 = \widetilde{R}_0 \bullet \widetilde{R}_2 = 3\mu(\mu+2)\left(\Delta x_1^2 + \Delta y_1^2\right),$$

$R_7 = \widetilde{R}_0 \bullet \widetilde{R}_3 = 3\rho(\mu+2)(\Delta x_1 \Delta x_3 + \Delta y_1 \Delta y_3)$,
$R_8 = \widetilde{R}_0 \bullet \widetilde{R}_4 = -2(\mu+2)\left((2\rho+1) \ (\Delta x_1 \Delta x_3 + \Delta y_1 \Delta y_3) + (2\mu+1)\left(\Delta x_1^2 + \Delta y_1^2\right) - (\Delta x_1 \Delta x_2 + \Delta y_1 \Delta y_2)\right)$,

$$R_9 = \widetilde{R}_1 \bullet \widetilde{R}_2 = 3\mu(\rho+2)(\Delta x_1 \Delta x_3 + \Delta y_1 \Delta y_3),$$

$$R_{10} = \widetilde{R}_1 \bullet \widetilde{R}_3 = 3\rho(\rho+2)\left(\Delta x_3^2 + \Delta y_3^2\right),$$

$$R_{11} = \widetilde{R}_1 \bullet \widetilde{R}_4 = -2(\rho+2)\left((2\mu+1) \ (\Delta x_1 \Delta x_3 + \Delta y_1 \Delta y_3) + (2\rho+1)\left(\Delta x_3^2 + \Delta y_3^2\right) - (\Delta x_2 \Delta x_3 + \Delta y_2 \Delta y_3)\right),$$

$$R_{12} = \widetilde{R}_2 \bullet \widetilde{R}_3 = 9\mu\rho(\Delta x_1 \Delta x_3 + \Delta y_1 \Delta y_3),$$

$$R_{13} = \widetilde{R}_2 \bullet \widetilde{R}_4 = -6\mu\left((2\mu+1)\left(\Delta x_1^2 + \Delta y_1^2\right) + (2\rho+1)(\Delta x_1 \Delta x_3 \ + \Delta y_1 \Delta y_3) - (\Delta x_1 \Delta x_2 + \Delta y_1 \Delta y_2)\right),$$

$$R_{14} = \widetilde{R}_3 \bullet \widetilde{R}_4 = -6\rho\left((2\rho+1)\left(\Delta x_3^2 + \Delta y_3^2\right) + (2\mu+1)(\Delta x_1 \Delta x_3 + \Delta y_1 \Delta y_3) - (\Delta x_2 \Delta x_3 + \Delta y_2 \Delta y_3)\right).$$

Iqra Saeed *is a Lecturer in the Department of Mathematics, Kinnaird College, Lahore.She has keen interest in the computer aided geometric design and data visualization.She has computed some good results about the theory of minimal surfaces..*
https://orcid.org/0009-0009-0116-0309.

Maria Hussain *is an Associate Professor of Mathematics in the Department of Mathematics, Lahore College for Women University, Lahore.Her research interest includes geometric modelling and data visualizatioin. She has contributed several results about free form curves and surface drawing techniques for geometric modelling and data visualization. She has special interest in curriculum design.*
https://orcid.org/0000-0002-4403-8997.

Hafiz Abdul Wajid *is a Professor of Applied Mathematics in the Department of Electrical Engineering at the Faculty of Engineering, Islamic University of Madinah, Saudi Arabia. His research focuses on mathematical modeling and data analytics. He has contributed to both theoretical developments and applied methodologies addressing challenges in modeling dependence structures and data-driven systems across interdisciplinary applications. He is also actively involved in faculty development, student advising, curriculum design for outcome-based education and ABET accreditation..*
https://orcid.org/0000-0003-1690-0823.

An International Journal of Optimization and Control: Theories & Applications (https://accscience.com/journal/ijocta)

This work is licensed under a Creative Commons Attribution 4.0 International License. The authors retain ownership of the copyright for their article, but they allow anyone to download, reuse, reprint, modify, distribute, and/or copy articles in IJOCTA, so long as the original authors and source are credited. To see the complete license contents, please visit http://creativecommons.org/licenses/by/4.0/.